MEASUREMENT OF LIQUID FILM THICKNESS IN HIGH ENERGY GAS-LIQUID TWO-PHASE FLOW

ZULFADZLI RIDZUAN

FACULTY OF ENGINEERING
UNIVERSITY OF MALAYA
KUALA LUMPUR

2019

MEASUREMENT OF LIQUID FILM THICKNESS IN HIGH ENERGY GAS-LIQUID TWO-PHASE FLOW

ZULFADZLI RIDZUAN

RESEARCH PROJECT SUBMITTED TO THE FACULTY OF ENGINEERING UNIVERSITY OF MALAYA, IN PARTIAL FULFILMENT OF THE REQUIREMENTS FOR THE DEGREE OF MASTER OF MECHANICAL ENGINEERING

FACULTY OF ENGINEERING
UNIVERSITY OF MALAYA
KUALA LUMPUR

2019

UNIVERSITY OF MALAYA
ORIGINAL LITERARY WORK DECLARATION

Name of Candidate: Zulfadzli Ridzuan

Matric No: KQK160022

Name of Degree: Master of Mechanical Engineering

Title of Project Paper/Research Report/Dissertation/Thesis ("this Work"):

Measurement of Liquid Thin Film Thickness in High Energy Gas-Liquid Two-Phase

Flow

Field of Study: Power Plant Engineering

I do solemnly and sincerely declare that:

(1) I am the sole author/writer of this Work;
(2) This Work is original;
(3) Any use of any work in which copyright exists was done by way of fair dealing and for permitted purposes and any excerpt or extract from, or reference to or reproduction of any copyright work has been disclosed expressly and sufficiently and the title of the Work and its authorship have been acknowledged in this Work;
(4) I do not have any actual knowledge nor do I ought reasonably to know that the making of this work constitutes an infringement of any copyright work;
(5) I hereby assign all and every rights in the copyright to this Work to the University of Malaya ("UM"), who henceforth shall be owner of the copyright in this Work and that any reproduction or use in any form or by any means whatsoever is prohibited without the written consent of UM having been first had and obtained;
(6) I am fully aware that if in the course of making this Work I have infringed any copyright whether intentionally or otherwise, I may be subject to legal action or any other action as may be determined by UM.

Candidate's Signature   Date:

Subscribed and solemnly declared before,

Witness's Signature   Date:

Name:

Designation:

MEASUREMENT OF LIQUID FILM THICKNESS IN HIGH ENERGY GAS-LIQUID TWO-PHASE FLOW

ABSTRACT

Gas-liquid two-phase flow is common on industrial application especially in refrigeration system and power plant such as the nuclear power plant. The objective of this study was to measure the liquid film thickness and flow profile in high energy gas liquid two-phase flow. The experimental two-phase flow vertical channel rig was installed with Constant Current Electrical Method (CECM) sensors, data acquisition (DAQ) and a high-speed camera to capture flow pattern and the hold-up (liquid film thickness). Experimental data were recorded for wide range of flow condition with specific combination of velocities of both phases, gas and liquid. At higher gas superficial velocity, flow pattern is moving from bubbly to slug to churn flow to annular flow, while at higher liquid superficial velocity, bubbles formations were very stable. Film thickness was observed to decreased as higher gas superficial velocity was introduced, and up to certain level, annular flow can be observed. At higher slip ratio, the film thickness value is almost constant as the flow has established a fixed pattern.

PENGUKURAN KETEBALAN FILEM CECAIR DALAM ALIRAN DUA FASA BERTENAGA TINGGI

ABSTRAK

Aliran dua fasa gas-cecair adalah aplikasi biasa dalam industri terutamanya dalam sistem penyejukan, dan loji janakuasa seperti loji tenaga nuklear. Objektif kajian ini adalah untuk mengukur ketebalan cecair filem dan profil aliran dalam aliran dua fasa gas-cecair bertenaga tinggi. Paip saluran menegak untuk eksperimen aliran dua fasa gas-cecair telah dibina dengan Kaedah Sensor Semasa Elektrik Berterusan (CECM), sistem pengambilalihan data (DAQ) dan kamera berkelajuan tinggi untuk mengambil gambar corak aliran dan data pecahan kekosongan. Data berangka dicatatkan untuk pelbagai keadaan aliran dengan gabungan halaju tertentu dari kedua-dua fasa, gas dan cecair. Pada halaju gas yang lebih tinggi, corak aliran bergerak dari aliran berbuih kepada aliran slug, seterusnya kepada aliran "churn" dan kepada aliran anulus, sementara pada halaju cecair yang lebih tinggi, gelembung terbentuk sangat stabil, dan sehingga tahap tertentu, aliran anulus boleh diperhatikan. Pada nisbah slip yang lebih tinggi, nilai ketebalan filem adalah hampir berterusan kerana aliran telah membentuk corak tetap.

ACKNOWLEDGEMENTS

I would like to express my deepest gratitude to my supervisor, Dr Mohd Zamri Zainon, for his invaluable guidance and advice, both in academics and in life. Thank you for being a great listener, for bestowing me the idea for this research and the flexibility of developing it.

Special thanks to my family, who have been with me through thick and thin, and for becoming the backbone that I need the most.

To my wife, Hanim Basarudin, I am truly blessed to have you as my life partner. Through our testing times, you stayed and held that pillar strong.

TABLE OF CONTENTS

LIST OF FIGURES

LIST OF TABLES

LIST OF SYMBOLS AND ABBREVIATIONS

CECM : Constant Electrical Current Method

CFD : Computational fluid dynamics

CHF : Critical heat flux

DNB : Departure form nucleate boiling

ECT : Electrical capacitance tomography

ERT : Electrical resistance tomography

FPS : Frame per second

LOCA : Loss of coolant accident

NR : Neutron radiography

A_C : Cross sectional area of vertical pipe

A_G : Cross sectional area of the core of the flow channel that filled by the gas phase

ρ_L : Density of liquid

ρ_G : Density of gas

D_G : Diameter of the core of the flow channel that filled by the gas phase

D_C : Diameter of the vertical pipe

z : Length of vertical pipe

$\dot{m}_L$: Mass flow rate of liquid

$\dot{m}_G$: Mass flow rate of gas

v_L : Mean velocity (Liquid)

v_G : Mean velocity (Gas)

LIST OF APPENDICES

CHAPTER 1: INTRODUCTION

The objective of this work is to measure liquid film thickness in high energy gas-liquid two-phase flow by using the Constant Current Electrical Method.

Gas-liquid two-phase flow in vast industries primarily those involving refrigeration or heat exchangers, such as power plants and nuclear reactors. One of the important aspects in gas-liquid two-phase flow study is the measurement of liquid film thickness, or hold-up. The characteristic of the liquid films is closely related to the performance and the safe operation of those system. It is important to have reliable measurement of hold-up to ensure plant operator have enough data and time for mitigation in the event of loss of coolant accident (LOCA) when the liquid film thickness becoming too small in a piping system. Furthermore, by having excellent information of liquid film thickness characteristic, engineers and designers can build safer and higher performing piping system.

Considerable amount of work has been carried out by researches to determine and improve the way of measuring and gather appropriate hold-up data in gas-liquid two-phase flow. Among developed methods are the theoretical method (Bretherton, 1961), the ultrasonic transmission technique (Kamei & Serizawa, 2002) and the laser extinction method (Utaka & Nishikawa, 2018). However, these techniques are limited to measurement of film thickness and can only be applied for certain cases of flow condition (Zainon, 2013). (Hewitt, 1978) measured the change of hold-up by making use of the change of conductance of two-phase mixture included in the space between a pair of sensor electrodes, however, there are some defect in this early work. This method has been further improved by (Fukano, 1998), by developing the Constant Electric Current Method (CECM), where it become the method to measure liquid film thickness in this work.

Therefore, to get most of the film thickness data to include wide range of flow conditions, the Constant Electric Current Method (CECM), developed by (Fukano, 1998), is used when several variables such as liquid superficial velocity and gas superficial velocity were to be considered into the measurement of the liquid film thickness and void fraction in the vertical gas-liquid two-phase flow. This method performed well and is highly reliable in the experiment.

CHAPTER 2: LITERATURE REVIEW

2.1   Two-Phase Flow in Pipes

Liquid are mostly stored in large containers of various shapes, cylinders, spheres and rectangular.

In the two-phase flow study, there are three discrete phases are accounted for. The phases are the gas, liquid and solid. The combination of any two of these phases, flowing co-current or counter current in a channel, is considered two-phase flow. It can be any combination of gas-liquid, liquid-solid, or gas-solid.

In general, there are three ways to explore the two-phase flow models. The first is an experimental approach where laboratory scales referring to industrial scales that is equipped with proper instrumentation as performed out by (Serizawa, 1974) and (Gardner, 1980).

The second method is by theoretical studies that are based calculation and correlation with the support of previous experimental data from early works such as (Mukherjee & Brill, 1983) and (Mora Vallejo & Zegrí, 2010)

The third, and most modern approach is by using analysis and modelling via Computational Fluid Dynamics (CFD). This is a method that is increasingly growing and has been speed up with development of latest computer technologies that allows faster and more reliable calculation of fluid dynamics. (Kataoka et al., 1987) and (Okawa et al., 2002) are among the researches that conducted excellent works based on this technique.
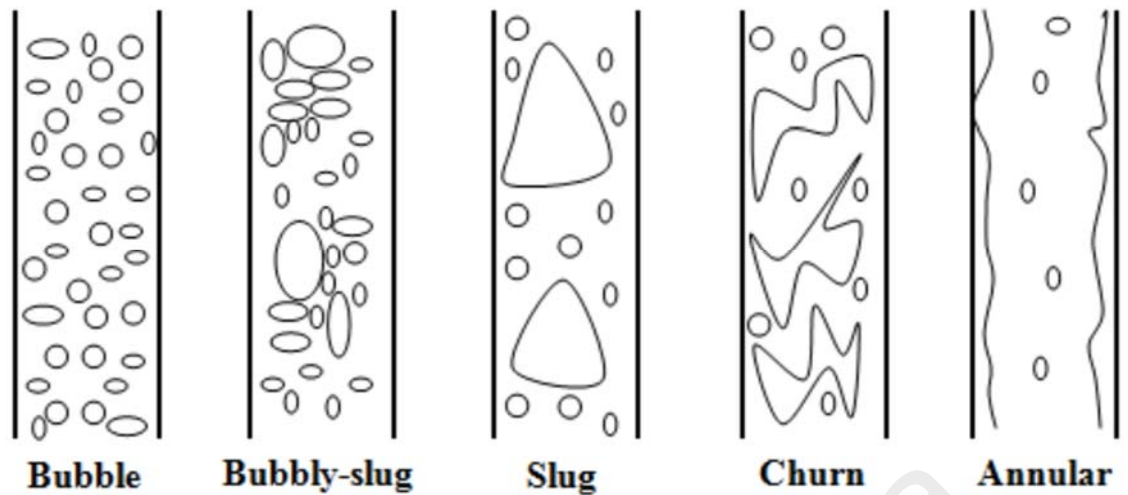
Figure 2.1: Gas-liquid two-phase flow pattern in vertical upward flow (Zainon, Zubir, & Ramli, 2014a)

Gas-liquid two-phase flow is formed when gas flowing in stationary or moving liquid in a flow channel. There will be bubbles existence and they are formed in many shapes and therefore creates various patterns for the whole flow channel. For vertical orientation, typical flow pattern can be mapped and clarified. The usual flow patterns recorded are bubbly flow, slug flow, churn flow and annual flow.

Having exceptional knowledge in gas-liquid two-phase flow is crucial for engineers and designers in industry that enables optimization of economics, operating condition and assessment of safety factors for the system (Zainon, 2013).

2.2   Void Fraction

Volumetric gas rate in the liquid flow can be considered the most important parameters to analyse the gas-liquid two-phase flow (Zainon et al., 2014a). It controls the estimation of the flow velocity and the two-phase density.

Void fraction in a gas-liquid two-phase flow can be defined as the fraction occupied by the gas phase to the channel cross-sectional area.

Void fraction can be calculated as the ratio of the gas volume, that is the ratio of the void in the channel to the total volume of the flow channel. Let's consider an adiabatic case with a mass flow rate, $\dot{m}_L$ of liquid, with density, ρ_L and mass flow rate, $\dot{m}_G$ of gas, with density, ρ_G are flowing upwards in a vertical pipe with diameter, D_C, length z, and cross sectional area, A_C.

Then by considering that equilibrium has been achieved the parameters in both phases can be treated as the following assumption, referring to Figure 2.2. In this case, the liquid mean velocity can be represented as v_L and the gas mean velocity as v_G, while the cross sectional area of the core of the flow channel that filled by the gas phase (void) represented as A_G and its diameter as D_G.
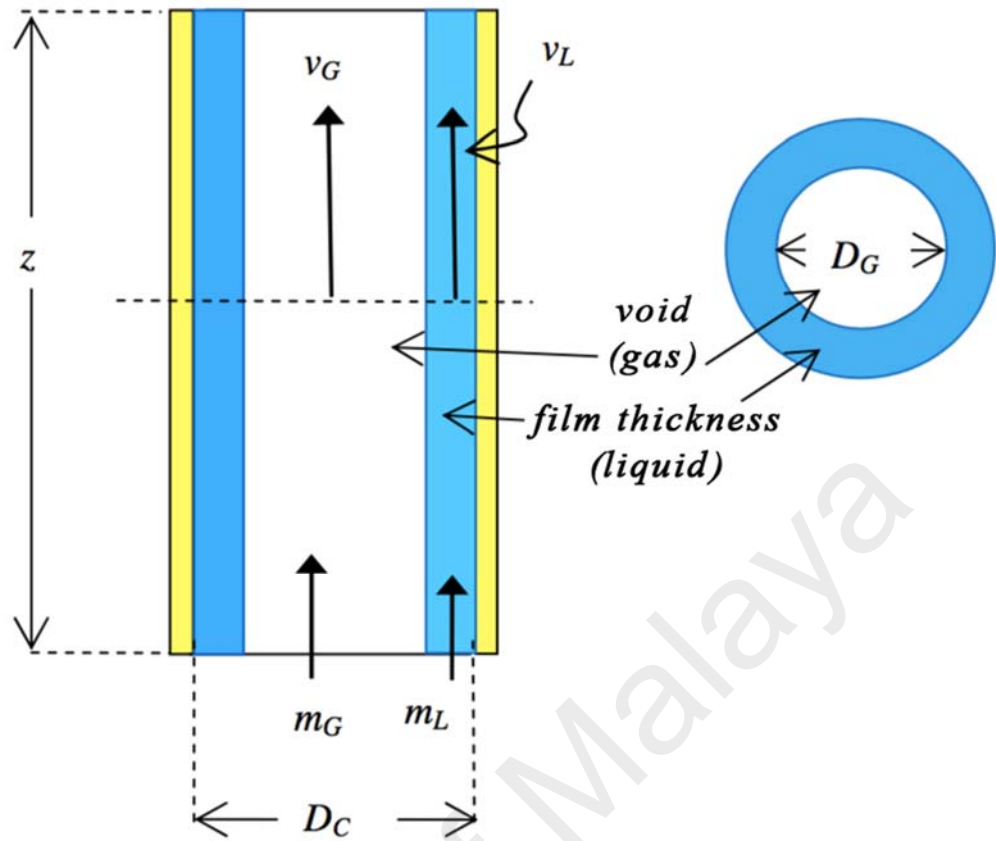
Figure 2.2: Fundamental depiction of void fraction

From Figure 2.2, the following relation can be established in order to describe the void fraction;

$$\alpha = \frac{A_G}{A_C} = \frac{1}{\left\{1 + \frac{m_L\,\rho_G\,v_G}{m\,\rho_L\,v_L}\right\}} \tag{2.1}$$

which can be simplified as;

$$\alpha = \frac{A_G}{A_C} = \left(\frac{D_G}{D_C}\right)^2 \tag{2.2}$$

17

On the other hand, the fraction for liquid area can be shown as;

$$\eta = \frac{A_L}{A_C} = \frac{m_L \, \rho_G \, v_G}{m \, \rho_L \, v_L} = 1 - \frac{A_G}{A_C} = 1 - \left(\frac{D_G}{D_C}\right)^2 \qquad (2.3)$$

The probability of finding gas at a given point can be determined using local probes, as the construction and placing of the probes will be describe in further details in section 3.3, Development of Sensor for Gas-Liquid Two-Phase Flow Measurement.

Although gas-liquid two-phase flow is widely used in industrial piping system, however, there is lack of possibility in industry for researches to visually observe the flow pattern or the mixture of the two-phase flow. To overcome this drawback, researches has developed techniques to investigate phenomena that occur in these piping systems by measurement of parameters such as void fraction and liquid film thickness.

Several techniques to measure void fraction has been developed such as the neutron radiography (NR) (Mishima & Hibiki, 2002), the conductance probes, impedance void meter, electrical resistance tomography (ERT) (Tan, Dong, & Wu, 2007), electrical capacitance tomography (ECT) (Sun, Liu, Li, & Lei, 2008), prediction method and Constant Electric Current Method (CECM) (Fukano, 1998).

In this work, the CECM method was applied to measure the liquid film thickness as well as void fraction and this method has excellent accuracy (Fukano, 1998) (Furukawa & Fukano, 2001) (Zainon et al., 2014b).

2.3   Liquid Film Thickness

To estimate the safety parameters in the annular regime of gas-liquid two-phase flow, it is crucial to study and have better knowledge of the liquid film thickness and its variation in gas-liquid two-phase flow.

The liquid film thickness can be applied as a guidance in determination of dry out point or burnout on the heating surface, in a system that involves heat transfer such as boiling and condensation. In early days, many accidents happened such as explosion in power plants due to lack of knowledge of critical heat flux (CHF), in terms of the mechanism and measurement. Since annular flow is the most common flow pattern in vertical gas-liquid two phase flow, predicting the CHF in annular gas-liquid two-phase flow is highly significant (Jiao et. al, 2009).

Dry out is a phenomenon that occurs when the film on the heated surface disappears due to evaporation and droplet formation. While the burnout in departure form nucleate boiling (DNB) is another phenomenon that occur when the thin liquid film beneath the vapor slug completely evaporate during the passage of slug bubble (Katto, 2011). In order to avoid dry out and burnout, the accurate knowledge of liquid film thickness is very important.

Liquid film thickness can be calculated by using the formula derived from void fraction measurement. Extracting from equation (2.3), the formula for the liquid film thickness can resolve but subtracting 1 to void fraction as define in equation (2.4).

$$\eta = 1 - \frac{A_G}{A_C} \tag{2.4}$$

CHAPTER 3: RESEARCH METHODOLOGIES

3.1 Development of Two-Phase Flow Rig

Gas liquid two-phase flow rig was constructed to simulate the actual industrial piping application. The top of the flow usually representing the actual condition in the industrial pipeline system.

A 1.2-meter length transparent pipe with inner diameter of 20 mm was constructed vertically. In between the length of the pipe, several electrodes (ring shape) were installed to suite the experiment needs.

Pre filtered water was supplied by a water pump, into the vertical channel from a 500-litre water reservoir completing one loop and recirculate through series of experimentation. The liquid flow was measured by a digital water flow meter and the fluid temperature was measured by thermocouple, which the temperature was maintained in between 28 °c to 31 °c.

At the bottom of the channel, air was injected from a compressor, measured using two type of flow meters, for low and high mass flow rate. Porous cap was installed at the tip of the gas line to produce fine bubbles into the mixing chamber. At this part, the air and water were mixed together and produce a gas-liquid two-phase flow vertically in the channel.
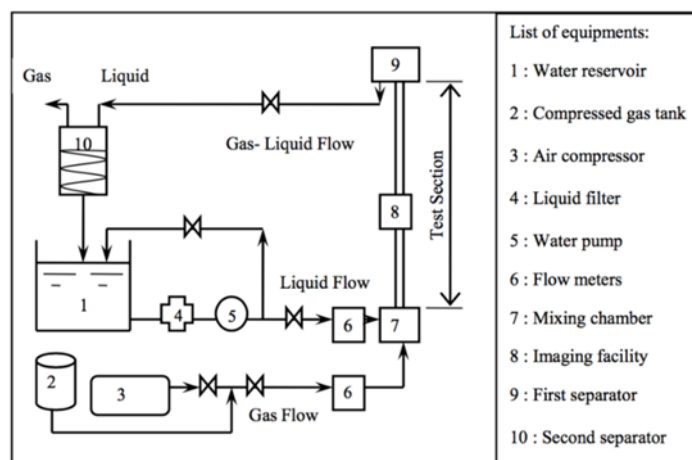

Figure 3.1: Schematic diagram of gas-liquid two-phase flow experimental facility (Zainon et al., 2014a)

3.2   Experimental Apparatus

There are two analyses conducted in this study, the flow pattern analysis and the measurement the void fraction and film thickness. For flow pattern analysis, visual inspection of bubble motion and fluid structure were studied using a high-speed camera, the Canon fast-cam Rabbit with capability of capturing image at 600 frame per second (fps). The Constant Electric Current sensor was then used to capture the voltage fluctuation during two-phase flow in order to obtain the value of void fraction and film thickness.

The experimental procedure can best be referred in detail from the flow chart that shows every steps of the process. Systematically, these works were divided into three categories, which are the development of the gas-liquid two-phase flow system, the flow pattern experiment and the development of sensor. Figure 3.2 shows the flow chart of the works.

The actual experimental facility is as shown in Figure 3.3. The test section was connected to the liquid and gas line at the bottom, where the two-phase flow fully formed in which the gas-liquid flow concurrently upwards and channelled back to the reservoir after passing through two separators at the top of the rig.

The data captured by the high speed camera and CECM sensors were recorded in real time throughout the experiment.
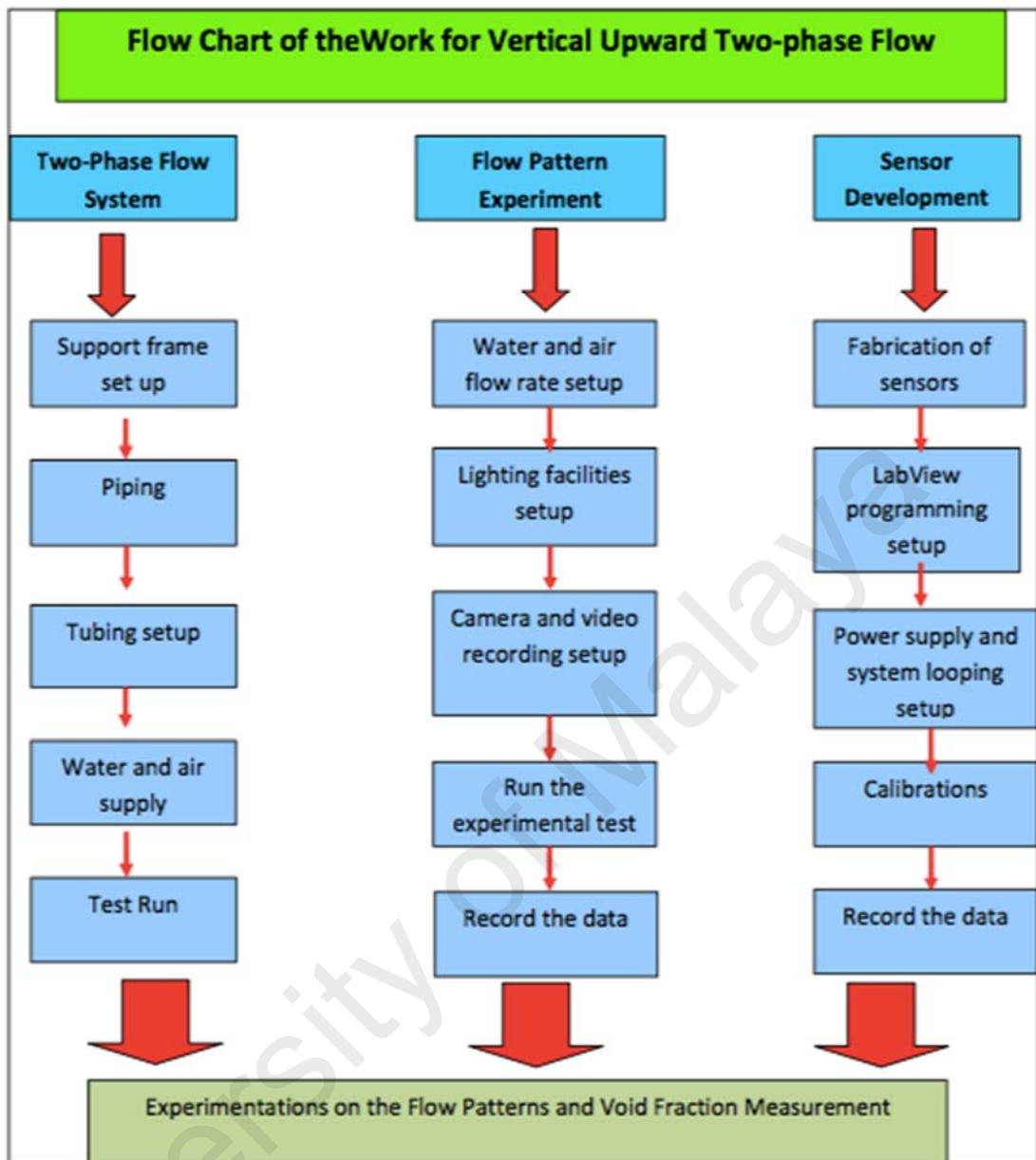
Figure 3.2: Flow chart for vertical upward gas-liquid two-phase flow experimental procedures (Zainon, 2013)

Figure 3.3: Experimental facility of vertical gas-liquid two-phase flow channel at Thermal-Hydraulics Lab, Department of Mechanical Engineering, University of Malaya.

3.2.1   Flow Pattern

In order to investigate the flow pattern, a high-speed camera was placed at the side of the vertical channel, assisted by two halogen lamps in the same visual direction to provide enough exposure so that the camera can provide adequate information in the picture taken. To capture the image of the bubble shapes and motion of the gas and liquid phase in the flow, the lamps and camera setup were placed at the centre of the flow channel, at Section II, in between the position of $L/D = 35$ and $L/D = 42.5$. The shutter speed of the camera is 600 fps.

The recorded video-graphic data of the flow patterns then were analysed, and the flow mapping process were carried out. The flow patterns, been recorded on graph sheets, were carefully differentiated according to variation of liquid and gas superficial velocities.

Gas superficial velocity, j_G was ranged between 0.025 m/s to 1.0 m/s and the liquid superficial velocities, j_L was ranged between 0.25 m/s to 2.0 m/s. Therefore, the range of slip ratio of velocities of the gas and liquid phases is $S = \frac{j_G}{j_L} = 0.01 \sim 4.0$. This range is a good approach for the application on industrial scale gas-liquid two-phase flow.

The results of different flow pattern based on variable gas and liquid superficial velocities are then discussed in detail in section 4.2.

3.2.2 Void Fraction and Film Thickness

The effect of axial location on the liquid film thickness and void fraction of the gas-liquid two-phase flow was studied where the flow channel was divided into three sections. The void sensor for Section I was placed at 400mm from the bubble injection making a normalised non-dimensional position at L/D=35, Section II at 300mm (L/D=42.5), and Section II (L/D=50). The value of voltage fluctuation during two-phase flow were taken from all four locations. The upper three void sensors are given more attention as the flow patterns are more stable in this area.

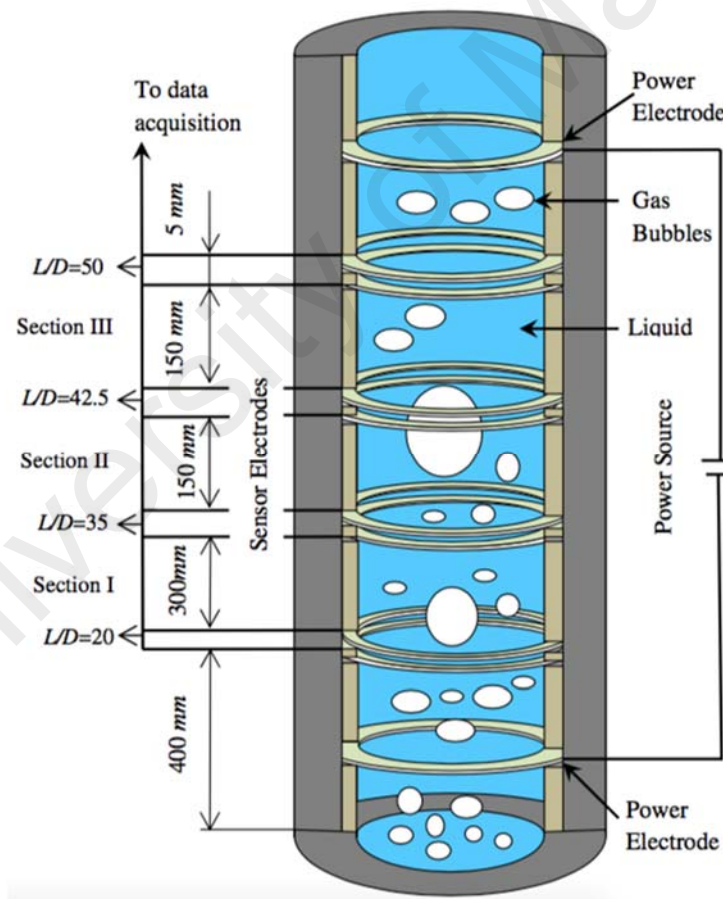Figure 3.4 shows the details of the sensor positioning and installation.

Figure 3.4: Detail configuration of the test section for vertical upward gas-liquid two-phase flow (Zainon, 2013)

3.3   Development of Sensor for Gas-Liquid Two-Phase Flow Measurement

3.3.1   Constant Electric Current Method (CECM)

Constant Electric Current Method (CECM) is type of conductance technique that can be installed around the vertical channel. The basic of CECM consist of a constant current power source and two types of electric conductance. A very low electric current was supplied via a pair of power source rigs placed at the bottom and top of the flow channel, and the other pairs is to detect the information of hold-up (η) or film thickness (Fukano, 1998). In this experiment, the conductance supplying the electrical power is called "Power Electrodes" and the conductance that detects the information of hold-up is called "Sensor Electrodes"

Basic equation of the CECM by using the electrical resistance concept, is as follows;

$$\frac{1}{R_{TP}} = \frac{1 - \eta}{R_G} + \frac{\eta}{R_L} \tag{3.1}$$

R_G is the resistance of the gas phase and R_L is the resistance of the liquid phase. The η is the hold-up, which is the percentage of the liquid volume to the total volume of the channel (Zainon et al., 2014b). This hold-up can be denoted as the film thickness of the respective measured region at the flow channel.

Using V_{TP} as the voltage drop in a unit length when a constant current I_0 is applied, the resistance should be $R_G \gg R_L$ for air-water two phase flow. In order to get the value of the hold-up (η), the equation can be expressed as;

$$\eta = \frac{R_L}{R_{TP}} = \frac{I_0 R_L}{I_0 R_{TP}} = \frac{V_L}{V_{TP}} \tag{3.2}$$

Here, V_L is the voltage output when there is no gas present in the measured cross section, and therefore when $V_L = V_{TP}$ the value of hold-up $\eta = 1$. Relating the above equation with void fraction as defined in section 2.2, calculating void fraction (α) from CECM method can be expressed as;

$$\alpha = 1 - \eta = 1 - \frac{V_L}{V_{TP}}$$
(3.3)

Hence, as described in Section 2.2 and 2.3, this sensor can be applied to study both the film thickness and void fraction. A further analysis performed by (Zubir et al., 2019) with this sensor as a prediction of the flow pattern via void fraction profile.

3.3.2   Construction of Sensors

The power electrodes and sensor electrodes can be fabricated by any good electrical conductor. For the current works, the electrodes were constructed using 0.5mm thick copper plate, with ring shape electrical conductivity at $\sigma = 5.96 \times 10^7 \; s/m$. These electrodes were constructed to suit with the channel diameter of 20 mm. These ring shape electrodes then installed in pair, with the distance of 5mm for one pair of sensor electrodes in the direction of the flow, embedded flush with the inner surface of the whole circumference of the channel. The sensor electrode pairs were placed at four locations along the vertical axis at 150mm distance between each other pairs. Configuration of CECM sensors is shown in Figure 3.5.
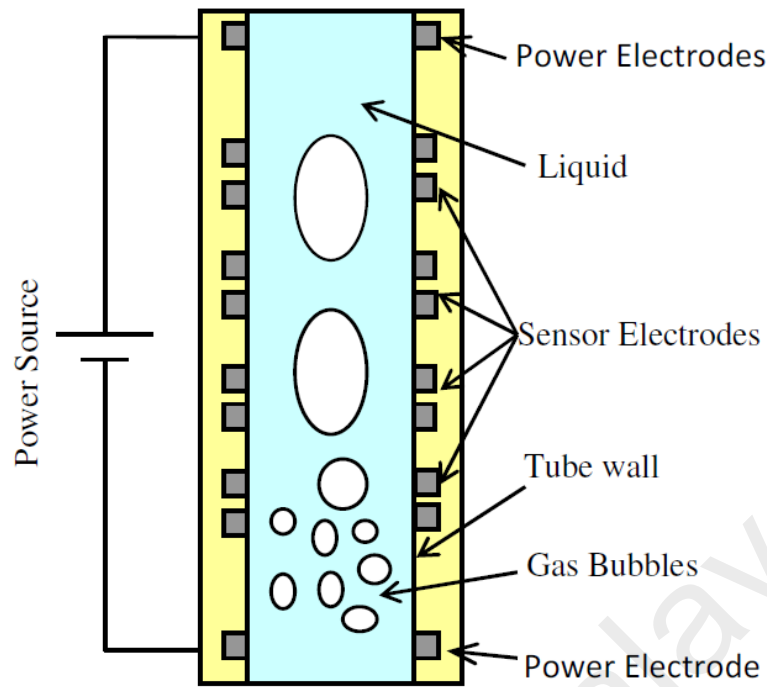
Figure 3.5: Schematic view of the configuration of CECM sensors (Zainon, 2013)

A constant electric current in the range of 0.1 ~ 0.3 mA was applied using a power source by GW Garner, model GPS 3030D. In order to avoid electrolysis on the electrode surfaces, a low direct current was considered since it can result in unnecessary gas bubbles in the flow channel. The outputs of the sensors were digitised using DAQ and sent to computer to further process the numerical data to determine the void fraction and film thickness.

3.3.3 Calibration of Sensors

Validation and reliability of these sensors are very crucial; therefore, calibration works were conducted based on two procedures, the static and dynamic method.

Static calibration was carried out by using a non-conductive rod with known diameter, to act as a gas bubble in the test channel. Cylindrical acrylic rods with four different diameters were inserted one after another on the channel filled with water. The voltage fluctuations then were calculated.

Based on equation (3.3), the hold-up (η) liquid film thickness was plotted on the graph, where a good error at 2% was obtained. Hence, this sensor shows a high degree of reliability.

Although static calibration is a good way of calibration for the sensors, it is however could not portrays the actual condition of the gas-liquid two-phase flow, due to the technique of using stationary position of the calibration rod.

The dynamic calibration in other hand was conducted by comparing visual data from the recorded images and measurement of the sensor. Single air bubble was injected using syringe through the bottom of the liquid filled channel, with difference needle size to produce different bubble size. Since in the channel only have single bubble flowing without any trails behind, therefore it can be confirmed that data captured by DAQ and camera focusing on a bubble only.

The dynamic calibrations were conducted at four different locations of sensors. The liquid superficial velocities were varied throughout the calibration procedure.

The image of the bubble was then analysed by measuring the size of the bubble in relative to the channel diameter. The size then was compared using calculation and data acquired via the sensor and DAQ. The dynamic calibration accuracy is within 3%

.

4.1   Outline of the Analyses

This chapter presents data acquired from the experimental procedure, as detailed in section 3.2. The following investigation results and discussions are considered;

    i.   Flow Pattern

    ii.   Film Thickness

The value of liquid superficial velocities and gas superficial velocities carried out in the experiment are as follows;

Table 4.1: List of gas and liquid superficial velocities

Liquid superficial velocities j_L (m/s)	Gas superficial velocities j_G (m/s)
0.25	0.025
0.50	0.050
0.75	0.075
1.00	0.100
2.00	0.150
2.50	0.250

The above velocities values are the manipulated variables in the three investigations stated above. The slip ratio for the above liquid and gas superficial velocities, calculated using the formula $S = \frac{j_G}{j_L}$ will be in between 0.1 to 3.0, which is a good approach to industrial scale gas-liquid two-phase flow.

Liquid superficial velocities were adjusted by inputting desired flow rate value into a digital control valve installed at the liquid supply pipe. The position of the valve is

at 1-meter length before entering the vertical channel. Gas superficial velocities were adjusted via a flow valve that was installed at the gas line before the vertical channel. Gas and liquid superficial velocities were calculated via the following equation;

$$V_{phase} = \frac{Q}{A} \tag{4.1}$$

Where V_{phase} is the superficial velocity, Q is the volume flow rate of the phase in $m^3 s^{-1}$ and A is the cross sectional area of the inner part of the vertical channel.

The instantaneous bubble velocities were analysed using the information from void fraction data using a computer programming. This code has capability to differentiate the peak values obtained from all the three locations of void sensors in time domain.

Therefore, the distance travelled by the bubbles (distance of sensors =150 mm) divide by the time taken from one location to another produce the values for velocities. The reference point taken on the bubble for calculating the distance is at the first void data triggered, which is at the topmost of the bubble.

4.2   Flow Pattern

The axial position of the camera, located at the centre of the vertical channel, is in the Section II. Referring to Figure 3.4, Section II is in between L/D=35 and L/D=45. From the experiment conducted, different flow patterns have been recorded via the high -speed camera as mentioned in section 3.2.1. These visual were analysed, and flow mapping was carried out.

Referring to Table 4.2, the flow pattern changes from bubbly flow, at $j_G = 0.025 m/s$ to churn flow at $j_G = 0.25 m/s$. At higher gas superficial velocity, the bubbles tend to coalesce together producing bigger bubbles, therefore moving towards the creation of churn flow, and finally annular flow.

At higher liquid superficial velocity, referring to Table 4.4 to 4.6, it is observed that the bubble flow formed was very stable around a wide range of gas superficial velocity. The bubble formed in this flow condition moving upwards steadily.

Liquid film still sticks on the wall of the channel at higher liquid superficial velocity, where at $j_L = 0.75 m/s$, the thickness of liquid film is considerable high although the flow has turned to churn flow at $j_G = 0.25 m/s$.

Table 4.2: Flow pattern at liquid superficial velocity, $j_L = 0.25 \ m/s$

$j_L = 0.25$ m/s	Gas superficial velocities, $j_G \ (m/s)$					
	0.025	0.050	0.075	0.10	0.15	0.25
Flow pattern						

Table 4.3: Flow pattern at liquid superficial velocity, $j_L = 0.5\ m/s$
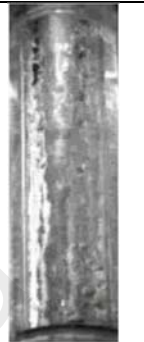
j_L = 0.5 m/s	Gas superficial velocities, $j_G\ (m/s)$					
	0.025	0.050	0.075	0.10	0.15	0.25
Flow pattern						

Table 4.4: Flow pattern at liquid superficial velocity, $j_L = 0.75\ m/s$

j_L = 0.75 m/s	Gas superficial velocities, $j_G\ (m/s)$					
	0.025	0.050	0.075	0.10	0.15	0.25
Flow pattern						

Table 4.5: Flow pattern at liquid superficial velocity, $j_L = 1.0\ m/s$

j_L = 1.0 m/s	Gas superficial velocities, $j_G\ (m/s)$					
	0.025	0.050	0.075	0.10	0.15	0.25
Flow pattern						

Table 4.6: Flow pattern at liquid superficial velocity, $j_L = 2.0\ m/s$

j_L = 2.0 m/s	Gas superficial velocities, $j_G\ (m/s)$					
	0.025	0.050	0.075	0.10	0.15	0.25
Flow pattern						

4.3   Film Thickness

Liquid film thickness can simply be defined as the hold-up (η) in the CECM calculation, where it can be defined as;

$$\eta = 1 - \alpha \tag{4.2}$$

Void fraction (α) calculation was derived from the formula derived in section 2.2. In this experiment, the data acquisition (DAQ) provides readings of void fraction directly from its software, LabVIEW®. Due to this condition, it is important to acquire the void fraction data, and using the formula stated above to determine the film thickness.

The data acquired was analysed at two different locations along the flow channel with axial position of L/D= 20 and L/D=35. The first position, L/D= 20 was set as the reference to check the responses of electric current in the flow hence obtaining the value of local film thickness at the beginning of the flow. The other position, L/D= 35 which is in the section II of the test section in Figure 3.4 were used in the overall calculations to obtain the hold-up η film thickness value.

Flow conditions were varied by changing the combination of gas and liquid superficial velocities as the pair listed in Table 4.1. The effect of flow conditions and axial positions to the liquid film thickness will be analysed and discussed in this section by plotting the average film thickness measurement over slip ratio, j_G/j_L , with varying liquid superficial velocity. These results were analysed by obtaining the trend and correlation between slip ratio and axial position to the variation of average film thickness value.

4.3.1 Local Average Film Thickness

In this section, the liquid film thickness that was recorded at two axial position, the L/D=20 and L/D=35. The measurement of average liquid film thickness is local at each location. Therefore, it is expected that different film thickness and flow characteristic will be eminent as the axial position is going higher. The results were plotted and analysed via several figures.
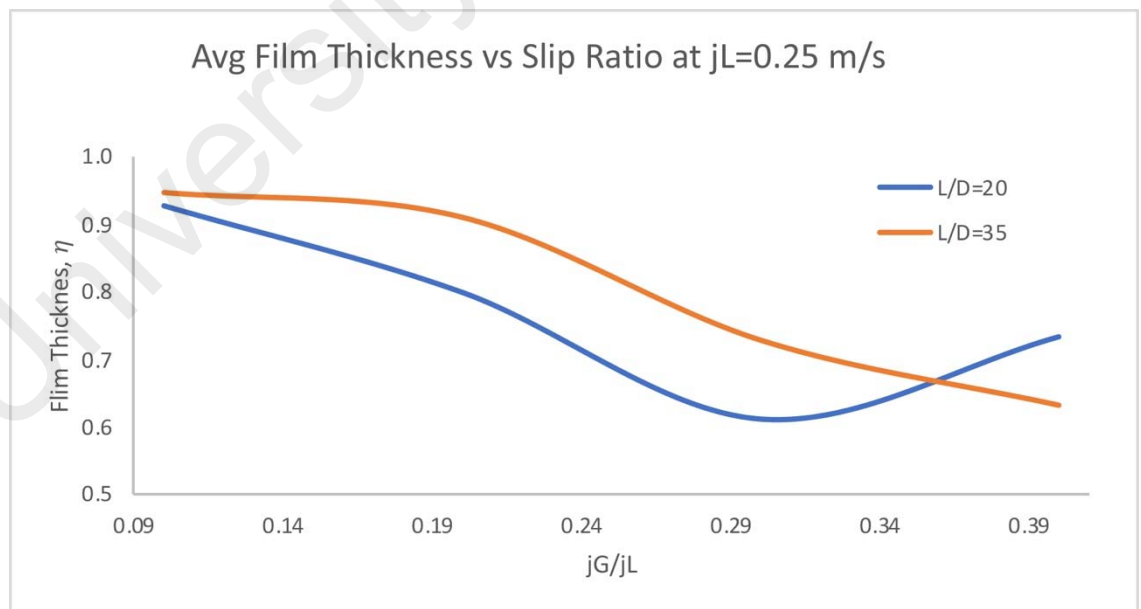

Figure 4.1: Average film thickness against slip ratio (S) at liquid superficial velocity of jL=0.25 m/s

Figure 4.1 shows the average film thickness against slip ratio for jL=0.25m/s. The vertical axis is the average film thickness (hold-up) and the horizontal axis is the ratio of the superficial velocity of gas to that of liquid. The average film thickness measurements were taken in the period of 10 seconds to better represent the overall hold-up η value. Figure 4.1 shows the comparison between L/D=20 and L/D=35 characteristic throughout the experiment. L/D=20 and L/D=35 are located at Section I and Section II respectively. Details on the position can be referred to Figure 3.4. At jL=0.25m/s, which the liquid superficial velocity is at the lowest in these experiments, film thickness at both L/D=20 and L/D=35 is decreasing as slip ratio increasing.

Both axial positions show that the average film thickness is decreasing as slip ratio increasing but the gradient started to change at slip ratio 0.29 where at L/D=35, the trend become gradual, towards smaller gradient.

It is observed initially that average film thickness is smaller at L/D=20 compare to L/D=35. However, for L/D=20, the average film thickness changed from decreasing with slip ratio to increasing with slip ratio at slip ratio 0.29.

Flowing further upward in the channel, the shapes of slug distorted, and become smaller, which shows at around slip ratio of about 0.35, average film thickness of L/D=20 surpassing L/D=35.
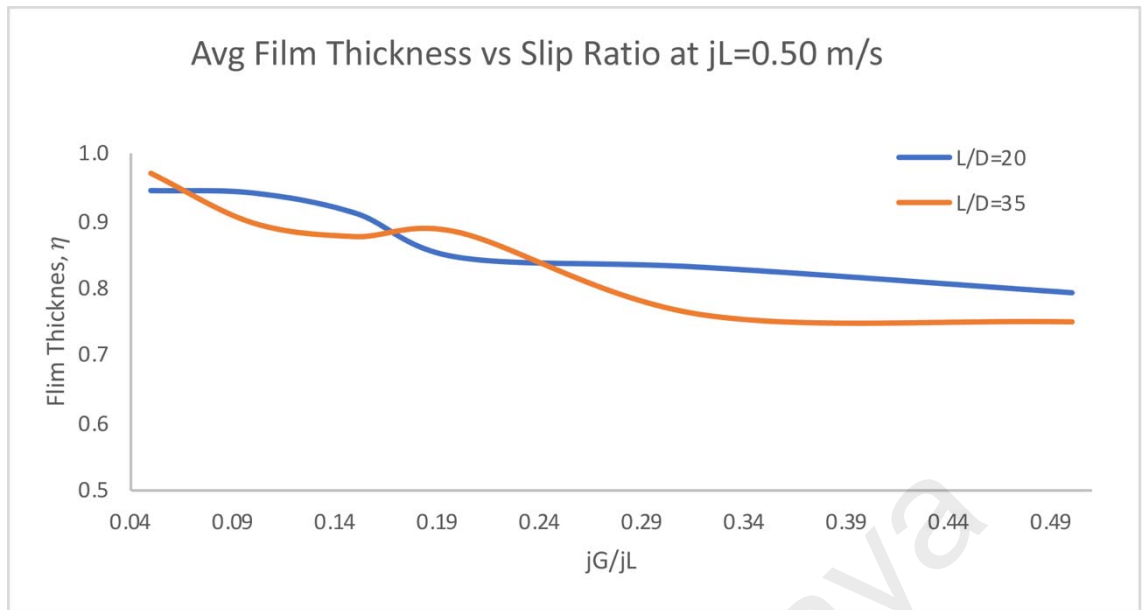
Figure 4.2: Average film thickness against slip ratio (S) at liquid superficial velocity of jL=0.50 m/s

In Figure 4.2, the liquid superficial velocity was adjusted to jL=0.50 m/s, which is higher than the results in Figure 4.1. It is clear that at this velocity, the average film thickness measured at L/D=20 and L/D=35 are alternately bigger and smaller compare to each other up to slip ratio 0.24. This pattern shows that at low gas superficial velocity, bubble characteristic at different axial position is hardly distinguishable.

Both positions recorded decreasing average film thickness as slip ratio increase. The average film thickness started to have steady measurement at slip ratio 0.29. Based on the trend in Figure 4.2, the slug in the flow will become stable in shape as gas superficial velocity increase and reach a stability point, hence showing an almost constant average film thickness throughout the rest of the higher slip ratio, suggesting that in the high slip ratio region, most of the flow have almost establish a fixed flow pattern.
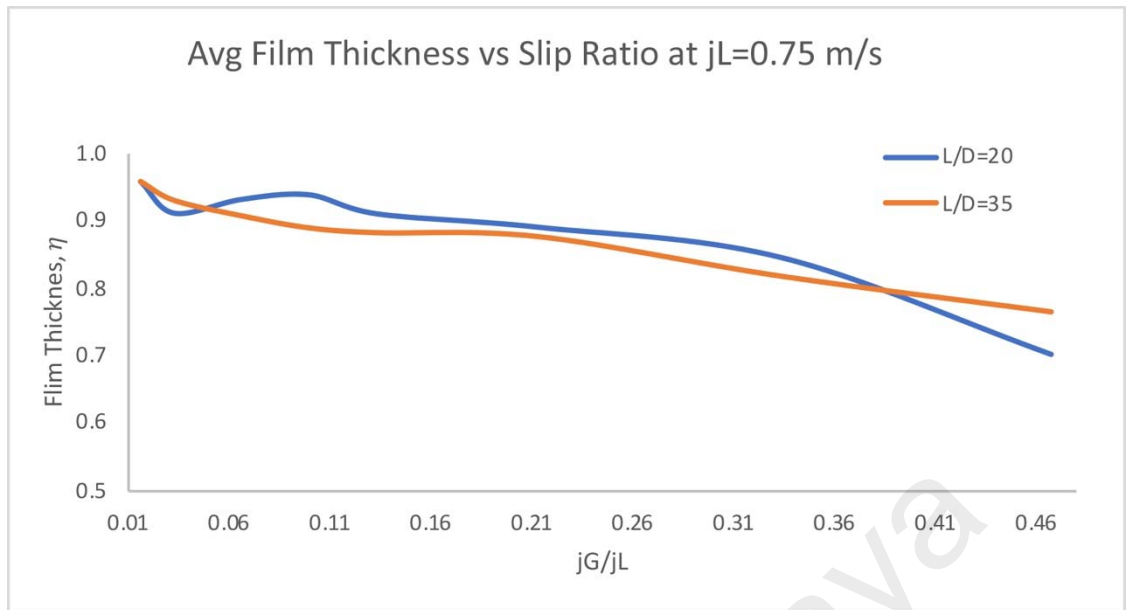
Figure 4.3: Average film thickness against slip ratio (S) at liquid superficial velocity of jL=0.75 m/s

The average film thickness in Figure 4.3 decreasing steadily with increasing slip ratio. At jL=0.75, the gradient of the is less than the one in Figure 4.1, where the liquid superficial velocity is lower. This shows that as the liquid superficial velocity increases, the average film thickness is stable, having less fluctuation between the maximum and minimum value. The measurement between L/D=20 and L/D=35 overlapped at around S=0.06 and S=0.38. For L/D=20, the average film thickness starts to decrease with steeper gradient at around S=0.38. At this point, average film thickness at L/D=20 was measured lower than the L/D=35. At higher axial position of the vertical channel, the average film thickness is steadily decreasing at a predictable pace and gentler slope.
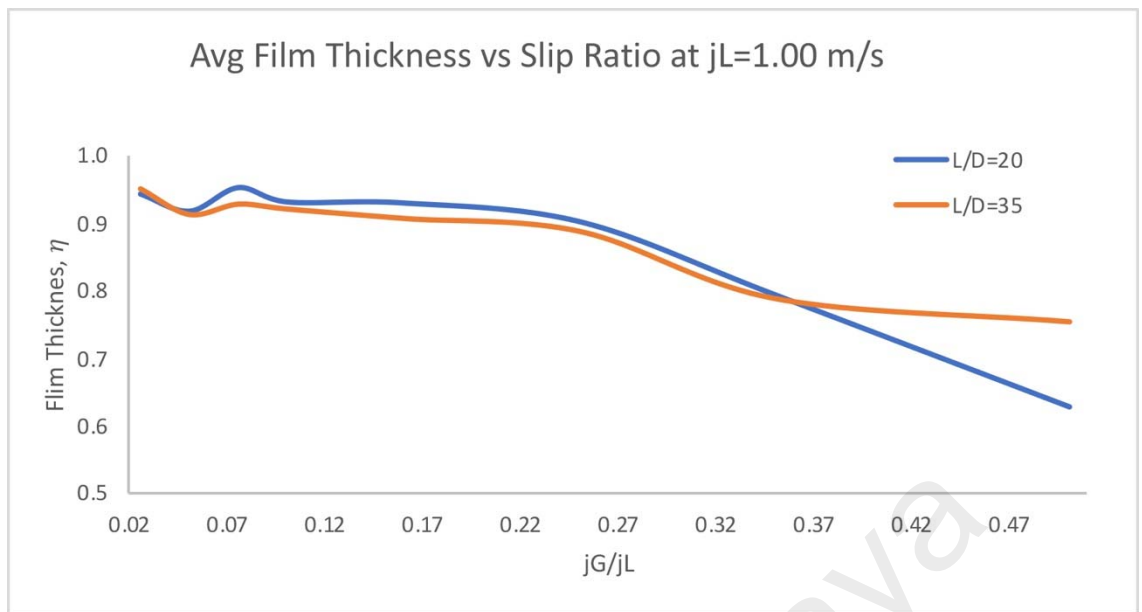
Figure 4.4: Average film thickness against slip ratio (S) at liquid superficial velocity of jL=1.00 m/s

Both L/D=20 and L/D=35 average film thickness was recorded producing almost the same pattern development in Figure 4.4, where the liquid superficial velocity is jL=1.00m/s. Initially, average film thickness was dropped until S=0.05 and rise up to maximum at S=0.07, then steadily dropping with gentle slope as the slip ratio increase. At around slip ratio S=0.37, the average film thickness at L/D=20 continues to drop with almost constant gradient. at L/D=35, the average film thickness starts to record constant almost flat trend.

Figure 4.5: Average film thickness against slip ratio at liquid superficial velocity of jL=1.50 m/s

Figure 4.5 shows a distinguishable average film thickness trend from previous figures with lower liquid superficial velocity. At jL=1.50m/s, both measurement at L/D=20 and L/D=35 do not overlapped each other, having a highly distinguishable trend, as if the two flows were completely different in flow pattern. At L/D=35, average film thickness was recorded high throughout the entire slip ratio between S=0.02 and S=0.11. Referring to Figure 4.1, Figure 4.2, Figure 4.3 and Figure 4.3, all the results makes it certain that the average film thickness will decrease as slip ratio increase. But for higher liquid superficial velocity of jL=1.50 m/s, at L/D=35, the average film thickness starts to increase at S=0.07 and the trend is moving upwards. However, at L/D=20, the average film thickness decreases at a steep gradient and gradually become gentler starting at S=0.03. The measurement continues to drop as slip ratio increases. The increases of liquid superficial velocity influence the characteristic of flow at higher axial position in the vertical channel, where average film thickness is observed to be increased regardless the effect of the increasing of gas superficial velocity.
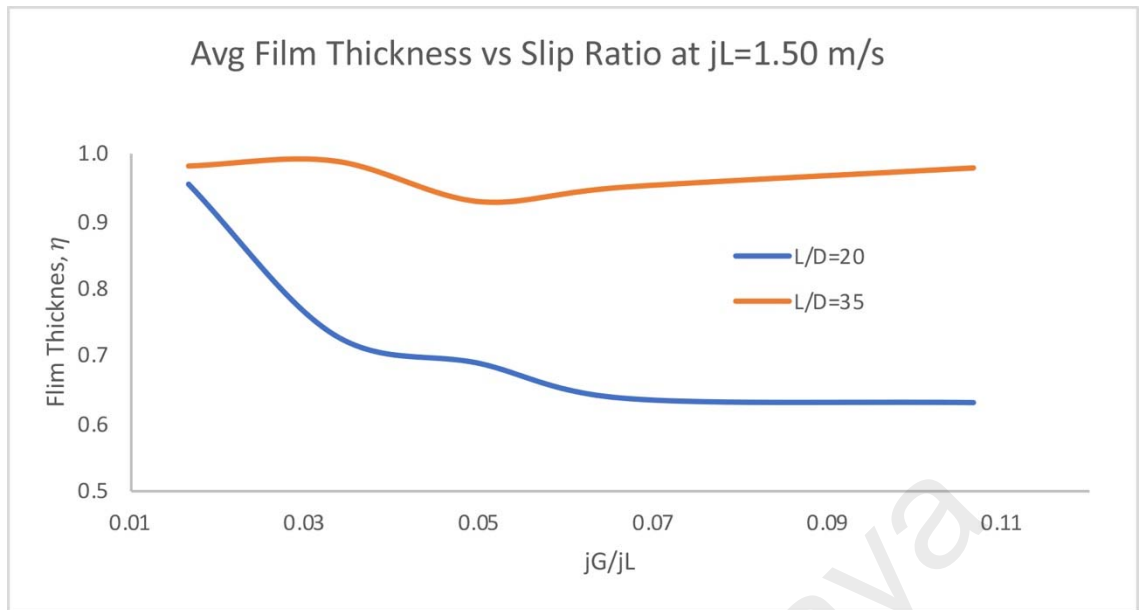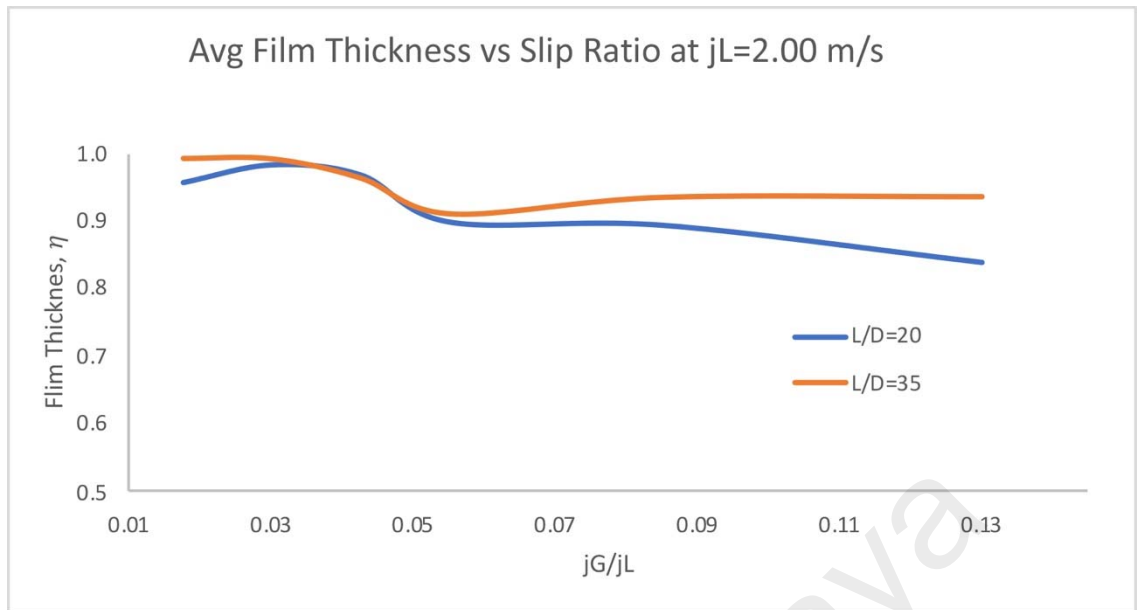
Figure 4.6: Average film thickness against slip ratio at liquid superficial velocity of jL=2.00 m/s

The average liquid film thickness in Figure 4.6 is recorded high at both L/D=20 and L/D=35 at liquid superficial velocity of jL=2.00m/s. The maximum value is 0.99 and minimum value of 0.62. Both axial positions have almost identical trend throughout the slip ratio. The data were overlapped in between S=0.03 and S=0.05. At this point, at both local position, flow pattern could be identical. The average film thickness starts to decrease a bit from S=0.05 to S=0.08, and started to decrease with gentle slope, almost flat to the end. This shows that as the liquid superficial velocity increases, the flow will have better ability to retain its film thickness relatively high despite the increase in gas superficial velocity. It is also very clear that at a really high liquid superficial velocity, the effect of gas superficial velocity to the film thickness is relatively low.
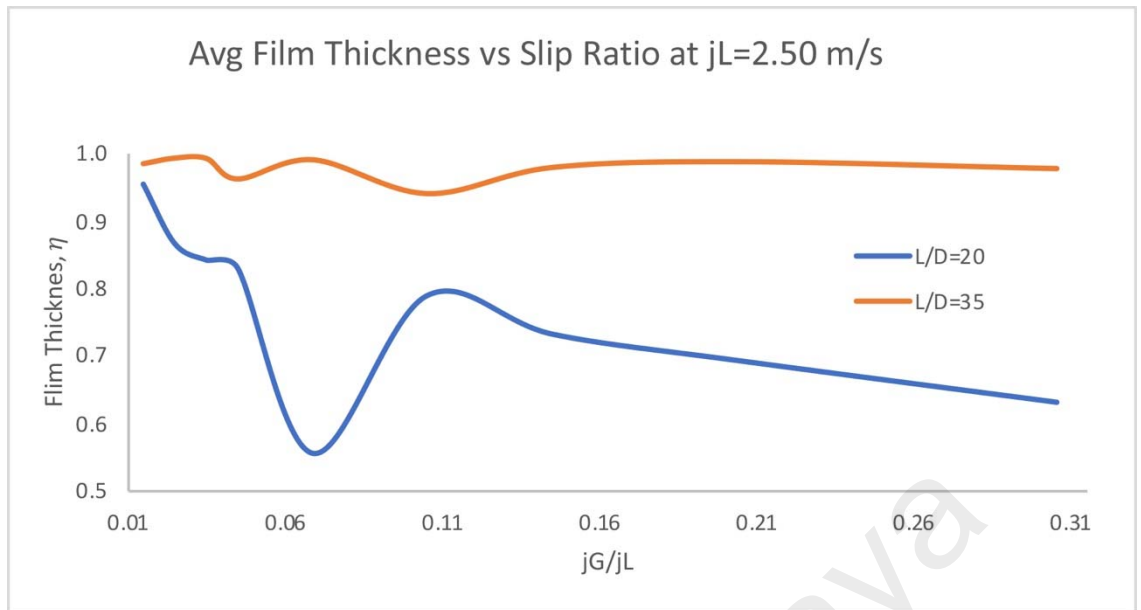
Figure 4.7: Average film thickness against slip ratio at liquid superficial velocity of jL=2.50 m/s

As the liquid superficial velocity increases to jL=2.50m/s, average film thickness is likely to maintain at high range. It shows clearly in Figure 4.7 where at L/D=35, the value of average film thickness drifts between 0.99 and 0.94. At lower axial position, the trend is not as stable. For L/D=20, the average film thickness dropped steeply at S=0.04 and regain higher value rapidly starting from S=0.07 up to S=0.11. Then the trend decreasing at a steady rate. Data trend, based in the effect of higher liquid superficial velocity as plotted in Figure 4.7 is synonymous with previous figures where at higher axial position, the average film thickness is higher and is stable as gas superficial velocity increase.

4.3.2   Average Liquid Film Thickness at Section I

Previous section discussed in depth about the changes in average film thickness measurement as the slip ratio increase, by manipulating the liquid superficial velocity. The analysis has made clear the different in average film thickness pattern between two axial position, that are L/D=20 and L/D=35. This is called the local measurement, at each sensor position.

However, in this section, the analysis will cover the average position of L/D=20 and L/D=35, to study the different characteristic of the liquid film thickness over the slip ratio, as liquid superficial velocity is manipulated. The results in this analysis will give better understanding of the characteristic of average liquid film thickness at Section I, the axial region between L/D=20 and L/D=35.

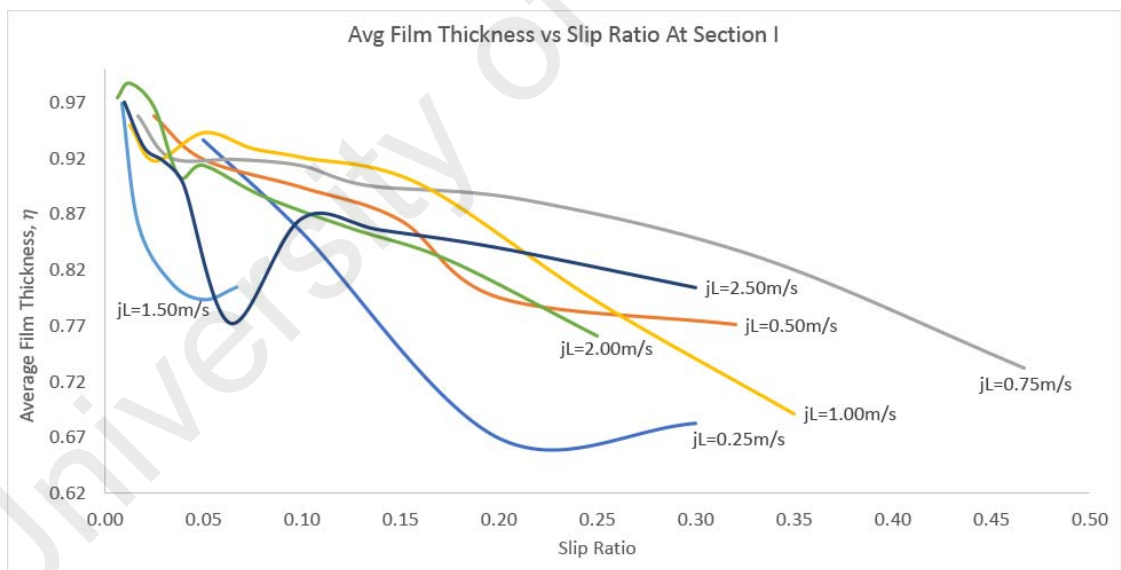**Figure 4.8: Average film thickness against slip ratio at Section I**

Figure 4.8 showing the effect of different liquid superficial velocity to the measurement of film thickness at the average value between L/D=20 and L/D=35, which is the Section I region of the test section.

There were seven different liquid superficial velocity were used in the test conducted. Between 0.25m/s to 1.00m/s, it is considered as relatively low velocity. Between 1.00m/s to 1.5m/s is medium velocity, and between 1.5m/s to 2.5m/s is considered as relatively high velocity.

For jL=0.25m/s, the average film thickness is decreasing over increasing of slip ratio. It shows stable measurement up to the lowest hold-up value of 0.67 at the slip ratio of 0.075, before the trend going up to hold-up value of 0.68. Increasing the velocity to jL=0.50m/s, the hold-up measured 0.96 gradually decreasing starting at slip ratio 0.05, and steepness is reduced at slip ratio 0.10. At slip ratio 0.15, the trend is decreasing steeper, before the value of slope starts to become smaller.

The pattern recorded for jL=0.75m/s is almost identical to jL=1.00m/s, where initially hold-up measurement was observed to decrease greatly. As it passes the slip ratio of 0.05, the gradient is less steep and gradually decreasing with gentle slope. Although falls within the medium velocity category as jL=1.00m/s, the hold-up measured at liquid superficial velocity of 1.50m/s shows very different pattern. Starting at 0.97, the hold-up was reduced drastically to 0.81 within short slip ratio.

Almost similar pattern observed in jL=2.50m/s. At this velocity, the hold-up value decreased steeply to 0.77 before climb with steeper slope to the hold-up value of 0.87. Falls within relatively high velocity category, jL=2.00m/s showing the same pattern. At slip ratio 0.04, the hold-up value drops significantly, before increase at steep slope, and continue decreasing gradually.

In all three categories, the average film thickness is observed decreasing as slip ratio increases. The measurement starts from hold-up value at almost 1 and gradually decreasing with different pattern recorded.

For relatively low liquid superficial velocity, initially up to the slip ratio of 0.15, the value of average film thickness is decreasing gradually. At the relatively high liquid superficial velocity, the gradient is steeper, almost vertical.

As the slip ratio increases, starting from 0.25, the measurement of average film thickness at all liquid superficial velocity shows steady decrease but for jL=1.50m/s and jL=0.25m/s, the measurement shows the trend is going upwards. These two velocities are in relatively high and low category.

These analyses can be concluded that at relatively high liquid superficial velocity, there will be huge drop in average liquid film thickness earlier as slip ratio increase, where the gas superficial velocity value is increases. But it will continue to stabilise and continue to reduce gradually.

At lower liquid superficial velocity, the trend is more stable. No huge drop and irregular trend can be observed.

CHAPTER 5: CONCLUSIONS AND RECOMMENDATIONS

The gas-liquid two-phase flow knowledge is highly important for engineers and designer to optimise their design to suit with economics requirement, operating condition and assessment of safety factors for the system.

Film thickness and void fraction measurement is crucial to avoid catastrophic accident such as departure from nucleate boiling (DNB) where if happens, plant meltdown is eminent.

The Constant Electrical Current Method (CECM) has proven to be a good setup to measure film thickness and void fraction with 2~3% accuracy and almost zero interference of the flow due to sensors were installed flush within the inner wall of the gas-liquid two-phase flow vertical channel.

The flow regime of the gas-liquid two-phase flow is changing from bubbly flow to dense bubbly flow, then slug flow, up to churn flow and finally annular flow as a higher gas superficial velocity was introduced. With the increasing of liquid superficial velocity, bubble formed was very stable.

Film thickness was observed to decreased as higher gas superficial velocity was introduced. As slip ratio increases, the flow may have established a fixed pattern, where the film thickness will be constant in high slip ratio region.

At a relatively high liquid superficial velocity, there will be huge drop in average liquid film thickness earlier as slip ratio increase, where the gas superficial velocity value is increases. The flow will eventually stabilised as slip ratio is increased further.

In this work however, there are several analyses and results that are abnormal in nature, such as in Figure 4.2, where value of film thickness of L/D=20 and L/D=35 is interchangeable as one is bigger than the other vice versa. While in Figure 4.3 and 4.4, where L/D35 shall have lower film thickness reading compared to L/D=20 but the slope was intercepted at 0.35 where film thickness for L/D=35 start to have higher value that the film thickness of L/D=20. Furthermore in Figure 4.7, where a huge drop in film thickness, then normalised as slip ratio increase.

All these anomalies in this work's results are highly recommended to be studied in future work, where the cause of these anomalies should be observed, analysed and recorded.

REFERENCES

Bretherton, F. P. (1961). The Motion of Long Bubbles in Tubes.

Fukano, T. (1998). Measurement of time varying thickness of liquid film flowing with high speed gas flow by a constant electric current method (CECM). *Nuclear Engineering and Design*. https://doi.org/10.1016/S0029-5493(98)00209-X

Furukawa, T., & Fukano, T. (2001). Effects of liquid viscosity on flow patterns in vertical upward gas-liquid two-phase flow. *International Journal of Multiphase Flow*, *27*(6), 1109–1126. https://doi.org/10.1016/S0301-9322(00)00066-5

Gardner, G. C. (1980). Fractional vapour content of a liquid pool through which vapour is bubbled. *International Journal of Multiphase Flow*. https://doi.org/10.1016/0301-9322(80)90002-6

Hewitt, G. F. (1978). Measurement of Two Phase Flow Parameters. In *Measurement of Two Phase Flow Parameters* (p. 111). Academic Press.

Jiao, B., Qiu, L., Lu, J., & Gan, Z. (2009). Liquid film dryout model for predicting critical heat flux in annular two-phase flow. *Journal of Zhejiang University-SCIENCE A*, *10*(3), 398–417. https://doi.org/10.1631/jzus.a0820322

Kamei, T., & Serizawa, A. (2002). Measurement of 2-dimensional local instantaneous liquid film thickness around simulated nuclear fuel rod by ultrasonic transmission technique. *Nuclear Engineering and Design*, *184*(2–3), 349–362. https://doi.org/10.1016/s0029-5493(98)00208-8

Kataoka, I., & Mamoru, I. (1987). Drift flux model for large diameter pipe and new correlation for pool void fraction. *International Journal of Heat and Mass Transfer*. https://doi.org/10.1016/0017-9310(87)90251-1

Katto, Y. (2011). Prediction of Subcooled Water Flow Boiling CHF over a Wide Range of Pressure. *Transactions of the Japan Society of Mechanical Engineers Series B*, *57*(542), 3449–3455. https://doi.org/10.1299/kikaib.57.3449

Mishima, K., & Hibiki, T. (2002). Development of high-frame-rate neutron radiography and quantitative measurement method for multiphase flow research. *Nuclear Engineering and Design*, *184*(2–3), 183–201. https://doi.org/10.1016/s0029-5493(98)00196-4

Mora Vallejo, L., & Zegrí, A. R. (2010). A Theoretical and Experimental study of Horizontal Air-Water. Two-phase Flow with a Spool Piece., (July). Retrieved from http://upcommons.upc.edu/handle/2099.1/14341#.WeYLYu9f0UA.mendeley

Mukherjee, H., & Brill, J. P. (1983). Liquid Holdup Correlations for Inclined Two-Phase Flow. *Journal of Petroleum Technology*, *35*(05), 1003–1008. https://doi.org/10.2118/10923-PA

Okawa, T., Kataoka, I., & Mori, M. (2002). Numerical simulation of lateral phase distribution in turbulent upward bubbly two-phase flows. *Nuclear Engineering and Design*. https://doi.org/10.1016/S0029-5493(01)00512-X

Serizawa, A. (1974). *Fluid-Dynamic Characteristics of Two-Phase Flow (Doctor of Engineering Thesis)*. Kyoto University. Retrieved from http://hdl.handle.net/2433/74984

Sun, M., Liu, S., Li, Z., & Lei, J. (2008). Application of Electrical Capacitance Tomography to the Concentration Measurement in a Cyclone Dipleg. *Chinese Journal of Chemical Engineering*, *16*(4), 635–639. https://doi.org/10.1016/S1004-9541(08)60133-0

Tan, C., Dong, F., & Wu, M. (2007). Identification of gas/liquid two-phase flow regime through ERT-based measurement and feature extraction. *Flow Measurement and Instrumentation*, *18*(5–6), 255–261. https://doi.org/10.1016/j.flowmeasinst.2007.08.003

Utaka, Y., & Nishikawa, T. (2018). Measurement of Condensate Film Thickness for Solutal Marangoni Condensation. *Journal of Enhanced Heat Transfer*, *24*(1–6), 279–290. https://doi.org/10.1615/jenhheattransf.v24.i1-6.200

Zainon, M. Z. (2013). *Effects of Vibration Onto The Flow Structures And Dynamics of Gas-Liquid Two-phase Flow (PhD Thesis). (PhD Thesis)*. University of Malaya.

Zainon, M. Z., Zubir, M. A., & Ramli, R. (2014a). Transition of Bubbly to Slug Flow in a Short Vertical Channel of Gas-Liquid Two-Phase Flow. *Advanced Materials Research*. https://doi.org/10.4028/www.scientific.net/amr.881-883.721

Zainon, M. Z., Zubir, M. A., & Ramli, R. (2014b). Velocities Effects on the Void Fraction Distribution in a Vertical Gas-Liquid Two-Phase Flow Channel. *Advanced Materials Research*. https://doi.org/10.4028/www.scientific.net/amr.889-890.369

Zubir, M. A., Ramli, R., & Zainon, M. Z. (2019). Determination of flow patterns in vertical upward two-phase flow channel via void fraction profile. *Journal of Applied Fluid Mechanics*. https://doi.org/10.29252/jafm.12.02.28351
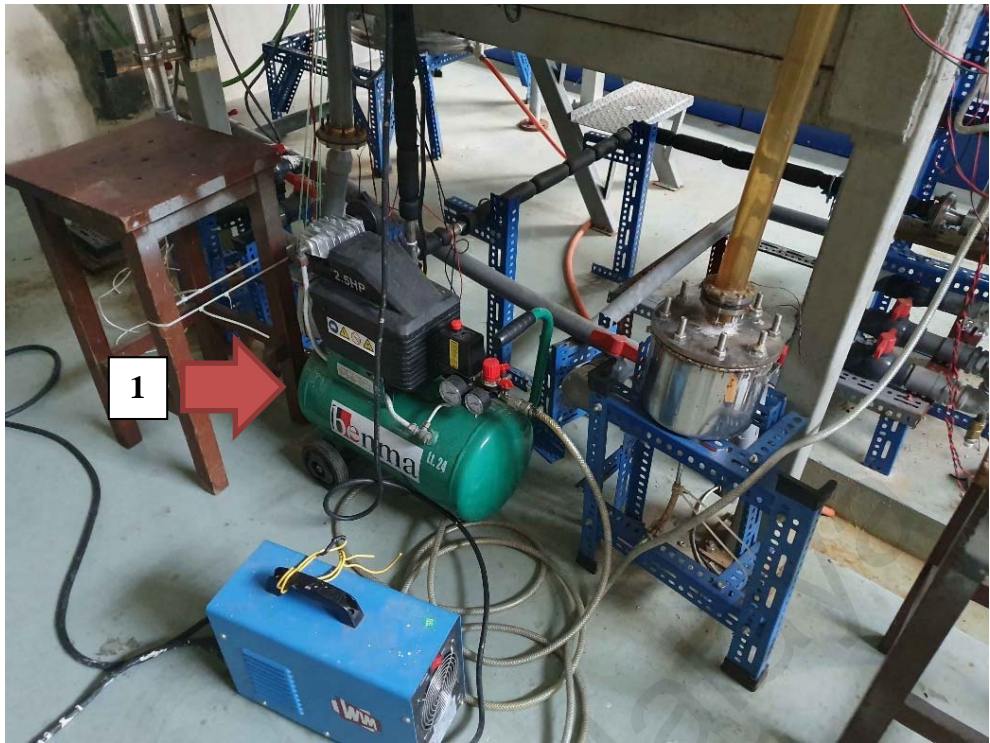
APPENDIX

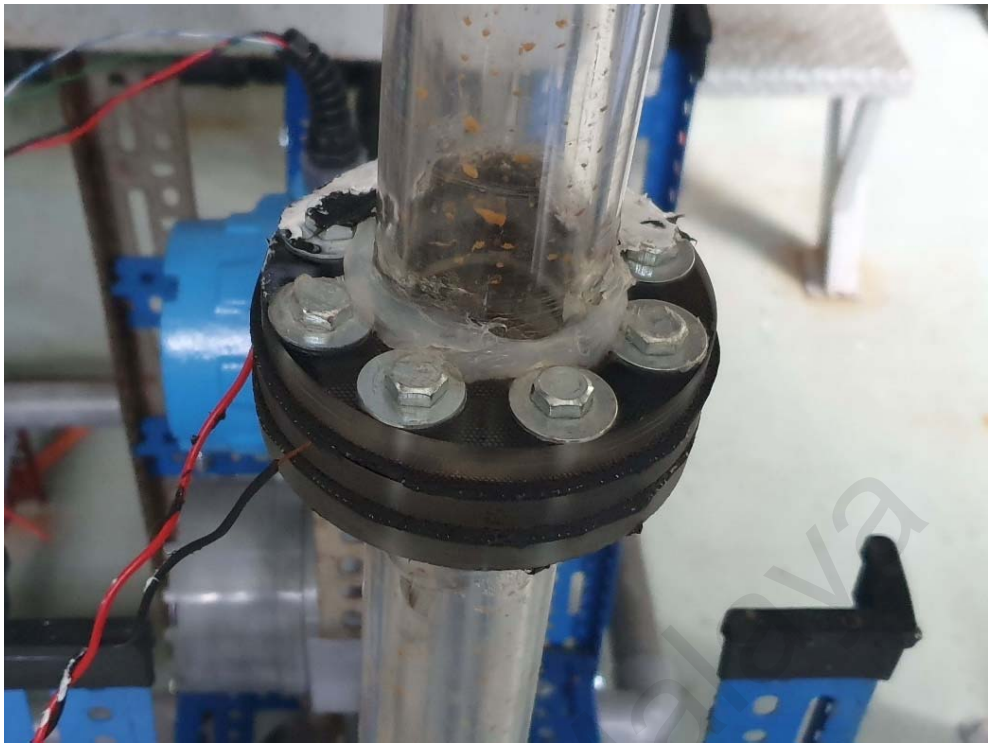
Appendix A: Air flow controller
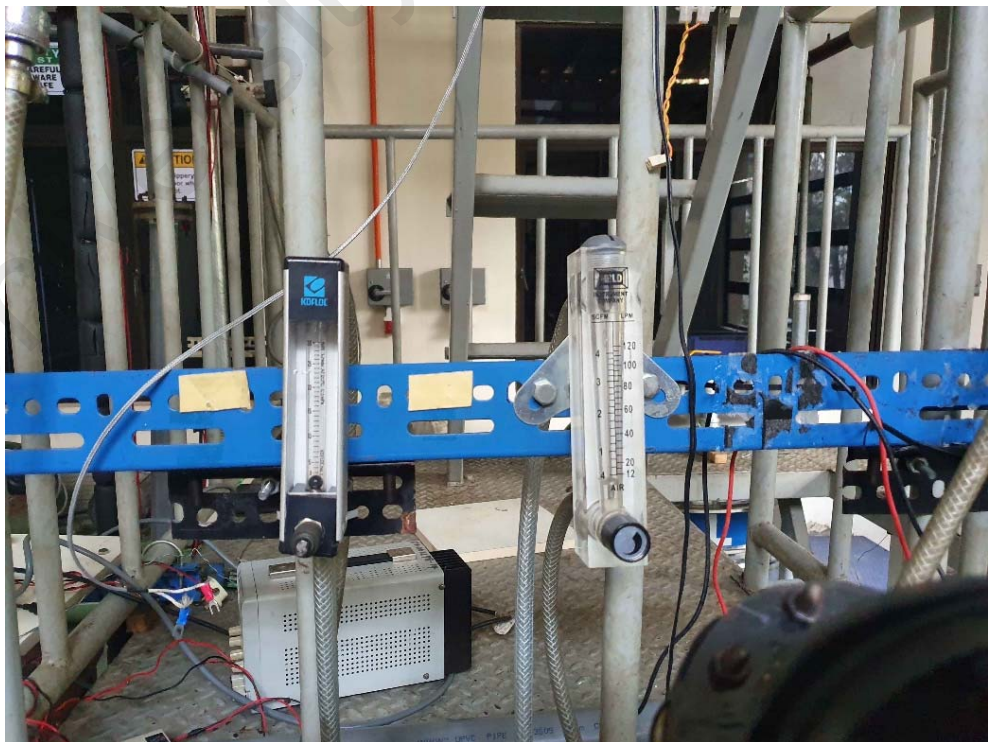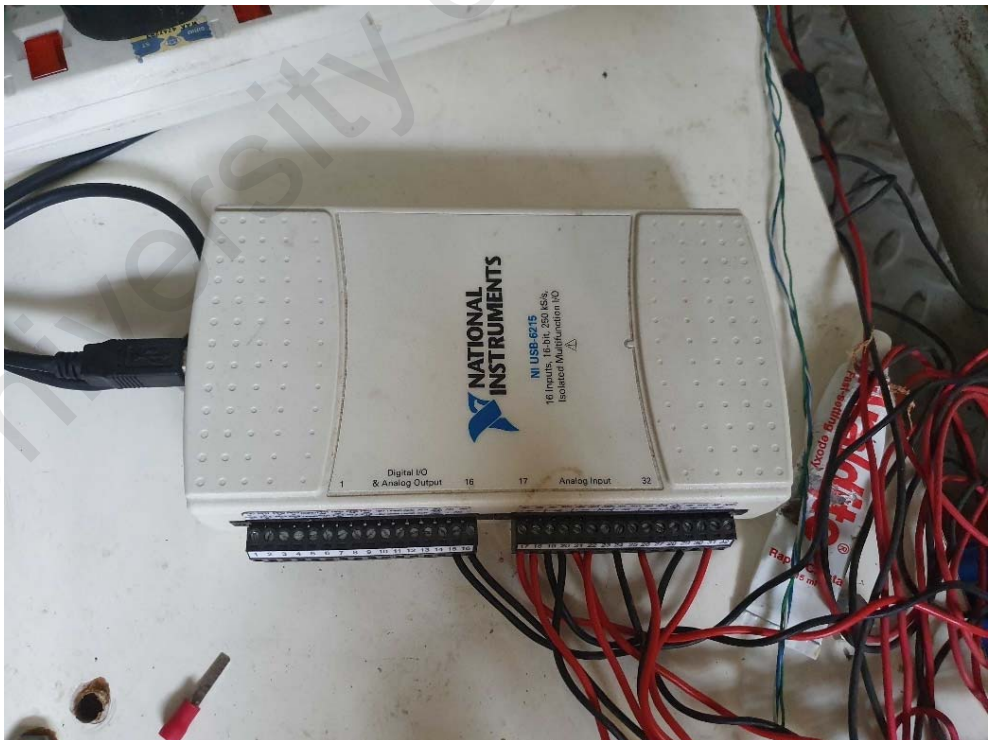

Appendix B: Air flow meter

Appendix C: Air compressor (1)

Appendix D: DC power supply, GW Garner Inc. (USA)

Appendix E: Sensor Electrode Assembly

Appendix F: National Instrument® data acquisition (DAQ)